Tropical analysis uncertainties and Kelvin waves: what can be learnt from the Aeolus wind profiles?

N. Žagar[1], M. Rennie[2]and L. Isaksen[2]

[1]Meteorologisches Institut, Universität Hamburg, Germany
[2]European Centre for Medium Range Weather Forecasts, Reading, UK

Key Points:

- Aeolus wind profiles improve tropical analyses in regions of a strong zonal wind shear in the tropical upper troposphere and lower stratosphere (UTLS).
- Aeolus winds are shown to modify the vertically-propagating Kelvin waves in UTLS.
- Impact of Aeolus winds in the ECMWF system in May 2020 is coupled to the easterly phase of the quasi-biennial oscillation.

Corresponding author: Nedjeljka Žagar, Meteorologisches Institut, Universität Hamburg, Germany,, nedjeljka.zagar@uni-hamburg.de

Abstract

The European Space Agency Earth Explorer mission Aeolus with the first spaceborne Doppler Wind Lidar onboard provides the global coverage of wind profiles twice per day. This paper discusses the impact of Aeolus winds on the quality of tropical analyses using the observing system experiments of the European Centre for Medium Range Weather Forecasts. Focusing on a period in May 2020, it is shown that Aeolus winds improve the fit of short-term forecasts to observations for other observations types, in spite of their random errors significantly greater than error estimates for short-term tropical forecasts. It is argued that Aeolus winds lead to more accurate representation of the vertically-propagating equatorial waves in the tropical upper troposphere. Examples of Kelvin waves suggest that analysis increments occur in the layers with a significant vertical shear during the easterly phase of the quasi-biennial oscillation in May 2020.

Plain Language Summary

Tropics are the region with the largest uncertainties in the initial state for numerical weather prediction - analyses. Analysis uncertainties are largest in the upper tropical troposphere and the lower stratosphere (UTLS). One of the reasons is a lack of wind profiles which are more useful than temperature profiles in the tropics. This classical effect was described by Smagorinsky as "Not all data are equal in their information-yielding capacity. Some are more equal than others". In this paper we show the impact of the first global wind profile observations by the ESA's mission Aeolus on the vertically-propagating Kelvin waves. Aeolus winds improve the structure of vertically-propagating waves in the UTLS in regions with the strongest wind shear. This effect is demonstrated on the Kelvin waves in May 2020 during the easterly phase of the quasi-biennial oscillation when shear lines in the tropical tropopause layer were particularly strong. In light of the previous work on the role of Kelvin waves in the tropical atmosphere and their treatment, or a lack of it, in tropical data assimilation modeling, lessons learnt from Aeolus winds can lead to improved assimilation procedures and a reduction of tropical analysis uncertainties.

1 Introduction

Even though progress in numerical weather prediction (NWP) in the past two decades has been tremendous (Bauer et al., 2015) including progress in the simulation of tropical variability (Vitart et al., 2014), the tropics remain a region with the largest analysis uncertainties, especially in the upper troposphere and lower stratosphere (UTLS); here, tropical analysis and short-range forecast uncertainties far exceed uncertainties in the upper-troposphere in mid-latitudes (Park et al., 2004; Žagar, 2017). For example, an inter-comparison of the six state-of-the-art NWP systems by Park et al. (2004) showed that the root-mean-square differences between the analyses over the tropics exceed the climatological standard deviation of the tropical circulation. In contrast, the differences among the same analyses over the extra-tropics make around 10% of the corresponding climatological variability. It is therefore not surprising that the description of synoptic variability in the tropical tropopause layer (TTL) is not reliable. Since variability of the tropical lower stratosphere is largely maintained by vertically propagating equatorial waves, their accurate representation in analyses is vital also for climate model validation (Fujiwara et al., 2012).

Analysis uncertainties in the tropics are associated with model errors, with shortcomings in data assimilation modelling and with a lack of observations, especially observations of wind profiles. In this paper we discuss a positive impact of the first spaceborne measurements of the global wind profiles by Doppler Wind Lidar ALADIN (ESA,

1999, 2008; Reitebuch, 2012), onboard the ESA Earth Explorer mission Aeolus[1] , on the quality of tropical analyses. We show that Aeolus wind profiles improve the fit of short-term forecasts to observations for other observations types, in spite of their random errors on average being significantly greater than error estimates for short-term tropical forecasts using the ensembles. We focus on analysis improvements in vertically-propagating equatorial waves in the UTLS region and specifically on the Kelvin wave. By filtering the Kelvin waves from the ECMWF analyses with and without Aeolus winds we demonstrate that Aeolus brings changes to the vertical wave structure in the layers with the strongest wind shear that is observed by Aeolus.

The Aeolus mission (Stoffelen et al., 2005) was under development since late 1990s leading to the successful launch of the Aeolus satellite in August 2018. At ECMWF, Aeolus observations have been used in operations since 9 January 2020. Prior to its operational use, a major effort was invested to validate the new measurements and to understand the origin of biases (Rennie & Isaksen, 2020, 2021). After the bias removal, the random error of Aeolus observations in clear air is still typically about twice that of radiosondes or aircraft wind measurements, because the effective Aeolus laser signal was a factor 2-3 lower than expected pre-launch. Nevertheless, evaluation of Aeolus forecast impact in the ECMWF operational system and observing system experiments show that Aeolus' impact on short-range forecasts has a similar magnitude to that of other satellite observations (Rennie & Isaksen, 2021), this in spite of Aeolus accounting for less than 1% of the assimilated observations. Forecast scores suggest that the largest positive impact of Aeolus winds is in the tropical UTLS region, with improvements in lower-stratosphere temperature forecasts extending to the medium range. Here we present the first evidence that reported improvements in the simulations of tropical circulation are associated with an improved representation of the large-scale equatorial waves in UTLS, in particular the Kelvin wave.

The Kelvin wave (KW) is one of the most studied features of the tropical atmosphere. The KW is the slowest eastward-propagating wave solutions of the linearized primitive equations and therefore the first-order ingredient of the circulation response to tropospheric heating perturbations (Salby & Garcia, 1987), easily detectable in different types of observations (Wheeler & Kiladis, 1999; Alexander & Ortland, 2010; Matthews & Madden, 2000; J. E. Kim & Alexander, 2013). In the stratosphere, where the KW was first discovered as a 15-day wave (Wallace & Kousky, 1968), it effects zonal mean quasi-periodic flows such as the quasi-biennial oscillation (QBO) (Baldwin & Coauthors, 2001), and it is widely considered to play a role in dynamics of the Madden-Julian Oscillation (MJO) (Zhang, 2005). Although the KW is predominantly a planetary-scale wave (zonal wavenumber 1), its analyses can still get occasionally poor even in the stratosphere (Podglajen et al., 2014).

In spite of its approximately non-dispersive nature and geostrophic coupling between the zonal wind the meridional pressure gradient, KW is a significant contributor to tropical analyses uncertainties and forecast errors, and its role in predictability has been addressed by several studies in the past (Žagar et al., 2007, 2013; Žagar, Buizza, & Tribbia, 2015). For example, Žagar et al. (2007) found that the ECMWF forecast errors within 20^o N-20^o S belt project on KWs significantly more in the easterly QBO phase than in the westerly phase. Žagar et al. (2016) showed that although the upper-troposphere tropical forecast errors grow more rapidly in the balanced modes, the analysis increments at the same levels are larger in unbalanced modes, including the KWs, than in balanced modes, suggesting shortcomings in the analysis of unbalanced tropical circulation. Furthermore, Žagar, Buizza, and Tribbia (2015) showed that missing variance in KWs explains a large part of underdispersiveness of the ECMWF ensemble prediction system in medium range in the tropics. It is unclear how well KW dynamics is

[1] `https://www.esa.int/Applications/Observing_the_Earth/Aeolus`

represented in global climate models, as they still poorly simulate the QBO and MJO, and their connections (H. Kim et al., 2020).

In a relatively short time since its launch, and in spite of larger systematic and random errors than expected pre-launch, Aeolus winds have justified and even exceeded expectations of atmospheric science community. This was only the case after the discovery of a strong link between onboard telescope temperatures and systematic wind speed errors (Rennie & Isaksen, 2020, 2021). Aeolus not only led to forecast improvements at several global NWP centres, but was also shown capable of observing gravity waves (Banyard et al., 2021) and providing useful aerosol observations (Baars et al., 2021).

Here we use a subset of the results from the ECMWF observing system experiments (OSEs) to investigate the tropical impact of Aeolus winds on process level. We suggest that Aeolus observations improve large-scale, vertically-propagating KWs by adding wind information in the layers of significant vertical shear of the horizontal winds in the tropical UTLS layer. In Section 2, we present the method including the evidence of a positive impact of Aeolus winds on the forecast fit to other observations types. Section 3 focuses on KW analyses, while Section 4 contains the discussion and outlook.

2 Method and Data

2.1 Observing System Experiment with Aeolus winds

ALADIN instrument onboard Aeolus measures four types of the profiles of the horizontal line of sight (HLOS) winds depending on the classification of atmosphere into clear air (Rayleigh winds) or cloudy (Mie winds) (D. Tan et al., 2008). Individual measurements with the scale of about 3 km are accumulated to produce profiles representative for up to 86 km scale for Rayleigh-clear, and about 12 km for Mie-cloudy scenarios. In the vertical direction, the atmosphere is divided into 24 layers, so-called range-bins, that have thickness 250-2000 m, and the HLOS wind is assigned to the center of the bin. Values of the Rayleigh-wind with large estimated observation error are rejected based on criteria 12 m/s (8.5 m/s) above (below) 200 hPa. After the bias removal, the random error of Aeolus observations in clear air is found to vary between 4 and 7 m/s for Rayleigh-clear winds and 2.8 to 3.6 m/s for Mie-cloudy winds (Rennie & Isaksen, 2021). The Rayleigh-clear winds below 850 hPa were discarded in these observing impact studies.

The OSE was performed for the Aeolus period May to September 2020 using the operational ECMWF system with 137 level up to 1 Pa. The model version was CY47R1.1 with the 4D-Var outer loop at resolution TcO399 which corresponds to about 30-km grid distance. The operational system applies the 12-hour continuous 4D-Var (Lean et al., 2021). The experiment which included Aeolus winds on top of all other observations is denoted "Aeolus". The reference experiment with all observations except Aeolus will be referred to as "NoAeolus". Rennie and Isaksen (2021) present the NWP impact assessment for the whole OSE period. Here we look at 12 UTC analyses during May.

An evidence of the impact of Aeolus winds is presented in Fig. 1 for a 10-day period, 20-30 May 2020, for the tropical belt 20^oS-20^oN. A relative improvement in the Aeolus experiment compared to NoAeolus is shown by the normalised root-mean-square-errors of the short-range forecasts compared to different observation types. This kind of assessment of forecast impact is more suitable than a comparison of forecast with analyses for a short period like here. We present the relative fit to zonal wind measurements from radiosondes, AMSU-A microwave radiances, and radio occultation (GPSRO) data, but we also computed (not shown) the fits for the aircraft, Atmospheric Motion Vectors (AMVs), and Japanese wind profilers. For all these observing systems there is a relatively large improvement in these independent observations, shown by values less than 100% in the error curves. The improved fit for the 20-30 May period is larger than seen from the same evaluation in the tropics over an extended period from April to September 2020

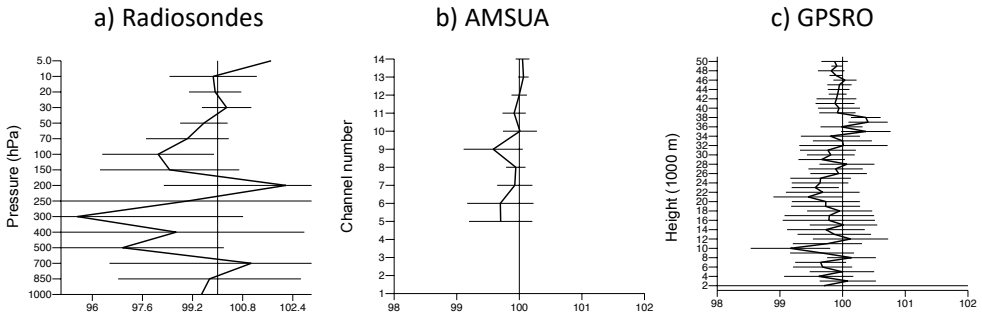

Figure 1. Root mean square errors for zonal winds in the tropics in period 20-30 May, normalised differences between the Aeolus and NoAeolus experiments. Evaluation is for background - observation for a) tropical radiosonde zonal winds, b) different AMSU radiance channels and c) GPSRO bending angle data. Values lower than 100% mean an improvement due to Aeolus winds. error bars. The error bars for 95% confidence intervals are included.

(not shown). Thus, Fig. 1 shows that using Aeolus winds generally improve forecasts and analyses.

2.2 Kelvin wave filtering

The KW is filtered from Aeolus and NoAeolus analyses using MODES (Žagar, Kasahara, et al., 2015) which implements classical linear wave theory in the terrain-following coordinate system following Kasahara and Puri (1981). MODES simultaneously projects winds and pseudo-geopotential field defined by temperature and surface pressure on balanced (Rossby) and unbalanced (inertia-gravity) eigensolutions of the linearized primitive equations. The framework is well suited for the KW which is the normal mode of the global atmosphere. For details of the linear wave filtering, the reader is referred to Kasahara (2020) and references therein. Filtering of operational ECMWF forecasts[2] reveals the KW signals regularly propagating eastward and upward to the stratosphere with the strongest tropospheric signal over the Indian ocean and western Pacific as illustrated in Supplement.

3 Aeolus winds and equatorial Kelvin wave

3.1 Kelvin wave winds versus balanced winds near the equator

KW zonal winds superposed on tropical balanced zonal winds in the NoAeolus and Aeolus experiments in mid-May 2020 are displayed in Fig. 2. The figure shows westerly winds in the upper tropical troposphere and within the TTL, except between 60^oE and 100^oE. In this region, KW winds are about equal or stronger than the balanced wind, which are also easterlies. The peak altitude of KW over the Indian ocean and in the vicinity of the strongest balanced easterlies are in agreement with the climatological KW structure in observations and in earlier ECMWF analyses (Suzuki & Shiotani, 2008; Alexander & Ortland, 2010; Flannaghan & Fueglistaler, 2013; Blaauw & Žagar, 2018). The associated KW temperature perturbations in TTL reach about 1.5 K (Blaauw & Žagar, 2018).

[2] `https://modes.cen.uni-hamburg.de`

An eastward-slanted, vertically propagating KW structure over the Indian ocean is in a contrast to a weaker KW signal over the western Pacific within a layer of balanced westerly flow below 100 hPa. Figures in Supplement show that KWs represent the most of the unbalanced (or non-Rossby) signal. The total zonal flow (Figures in Supplement) appears far less smooth than the balanced winds because small-scale, divergent structures project on the inertia-gravity modes. The predominant feature of Fig. 2 is a strong shear of the zonal wind, both vertical and horizontal. The presence of a strong easterly wind shear layer between 100 hPa and 80 hPa in May 2020 is associated with the easterly QBO phase which is known to provide favourable conditions for intense KW dynamics (Suzuki et al., 2010; Flannaghan & Fueglistaler, 2012).

Figure 2 also shows that between 13 May and 16 May 2020, balanced easterlies over the Indian ocean strengthened, along with strengthening westerlies around the dateline. An even stronger enhancement of both horizontal and vertical shear occurred in the total wind (Figures in Supplement). Such strong wind shear is typical for mid-latitude fronts with Aeolus demonstrated capable of improving their mesoscale features (Šavli et al., 2018). On synoptic scales in mid-latitudes, the thermal wind balance can be applied to derive the vertical wind shear from the horizontal temperature gradient, with the temperature field obtained from high-accuracy measurements of radiances. In the tropics, the weak-temperature gradient theory for the slow, large-scale motions relies on the smallness of temperature gradient (Sobel et al., 2001), thereby excluding the KW. However, wherever the Kelvin and Rossby waves are present together near the equator, their zonal winds will sum up (or subtract) whereas their temperature perturbations will subtract (or sum up), since their mass-wind couplings have opposite signs. Using the horizontal structure of mass-field observations to derive the Kelvin and Rossby wave signals near the equator therefore requires quantification of their respective variances. This is a challenging task for data assimilation, even in the perfect-model 4D-Var (Žagar, 2004). Direct wind observations, as argued since early days of the Aeolus project, are crucial to improve accuracy of tropical analyses.

3.2 Effects of Aeolus winds on Kelvin waves

There is little difference between the NoAeolus and Aeolus experiments in Fig. 2. An eye inspection suggest that differences are up to the level used for contouring, 3 m/s. This is not a small value for an experiment in which the only difference is the assimilation of Aeolus winds characterised by a significant random error. To understand tropical dynamical processes affected by Aeolus assimilation, we need to look at differences between analyses or at analysis increments. The latter shows the effect of observations in a single assimilation cycle whereas the former includes the effect of observations assimilated earlier in the experiment. The memory of observations in the tropics should be longer than in the extratropics (Fisher et al., 2005). Observations that affect the tropical mean state can be expected to have a memory of at least 10 days as it was seen for Aeolus data and AMSU-A radiance data in reanalyses (not shown). With the focus on Aeolus effects of vertically-propagating waves and their impact on circulation, we present differences between analyses with and without Aeolus winds.

Figure 3 shows that differences between KWs in the two experiments occur mainly over the Indian ocean at the locations of the vertical wave propagation and significant shear. For example, the assimilation of Aeolus winds on 13 May enhanced easterlies near 100 hPa over Indian ocean while on 19 May the KW vertical structure was modified over a deeper layer. Differences in the TTL are several meters per second. The vertical KW structure at two locations, 66^oE and 90^oE, and 3 consecutive days is presented in Fig. 4. It shows the downward propagation of the KW phase from the lower stratosphere across the TTL. The vertical phase speed at 66^oE earlier in the period has a greater amplitude than at 90^oE. The most relevant is the modification of the KW shear between 100 hPa and 50 hPa where the amplitudes and vertical propagation are the largest.

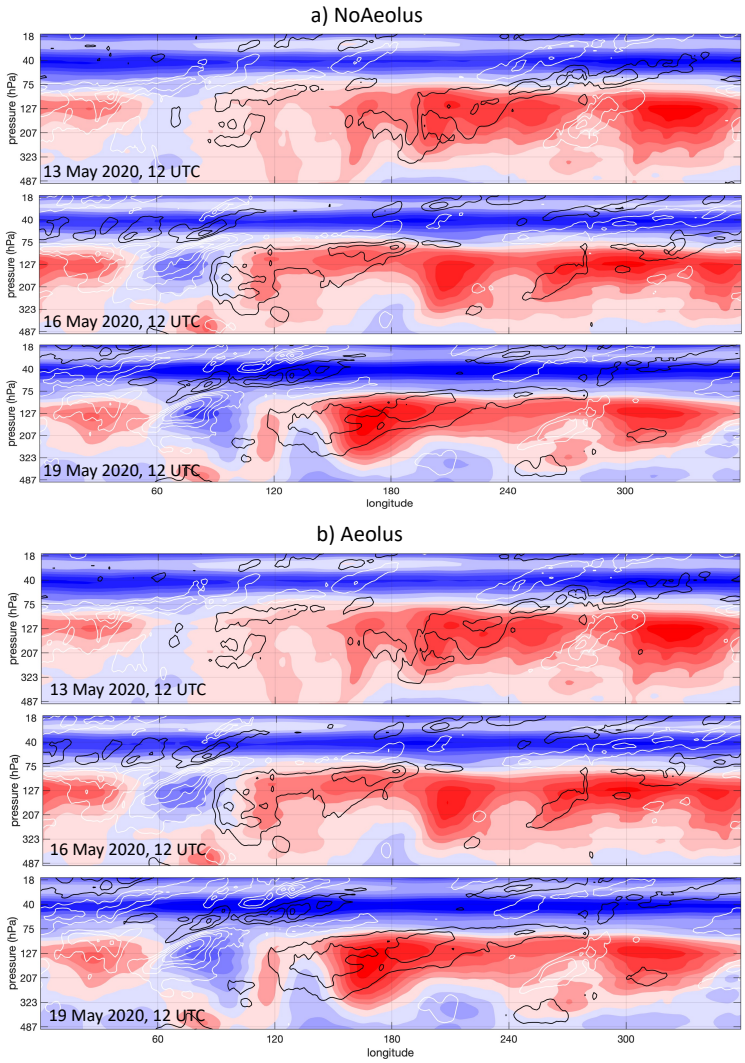

Figure 2. Kelvin wave zonal winds (contours) superposed on the balanced winds (shades) along the equator, averaged over the belt 10°N-10°S in (a) NoAeolus and (b) Aeolus experiments on 13 May, 16 May and 19 May 2020, 12 UTC. Contouring is every 3 m/s, starting at ±3 m/s, with black contours for westerly and white contours for easterly Kelvin wave winds. Balanced zonal winds is shaded every 3 m/s, with red shades for westerlies and blue shades for easterlies.

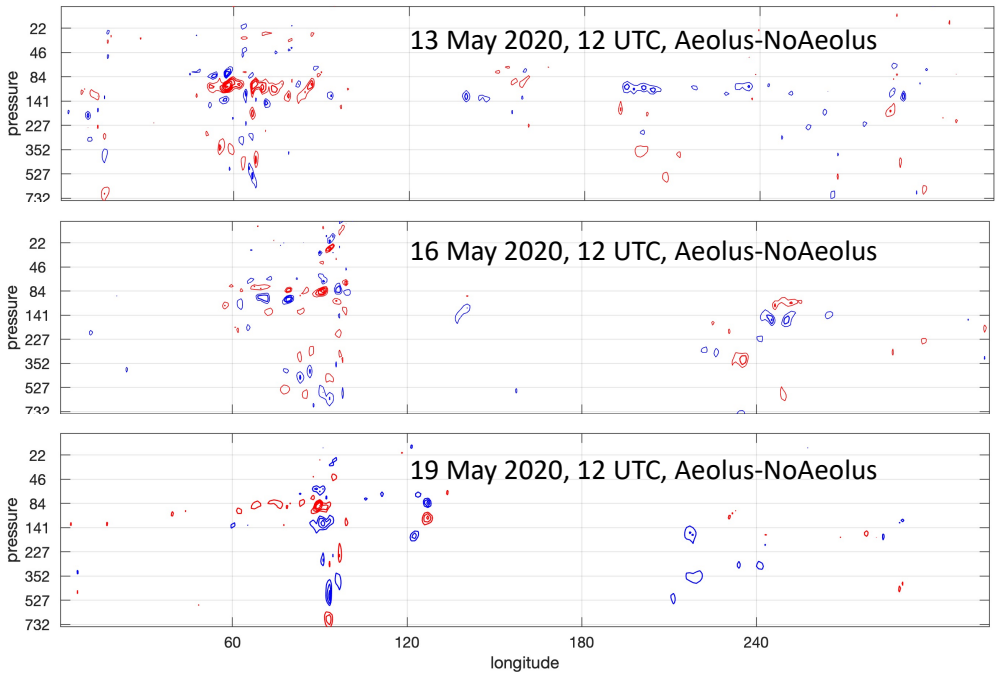

Figure 3. Kelvin wave zonal wind differences along the latitude 0.5^{o}N between the Aeolus and NoAeolus experiments on 13 May, 16 May and 19 May 2020, 12 UTC. Contouring is every 0.5 m/s, starting at ±1 m/s. Red contours for positive, and blue for negative differences.

In contrast to the large portion of the total zonal circulation associated with KWs (Fig. 2), its analysis increments are relatively small (not shown). This may suggest that KWs are well represented in forecasts (first-guess fields) in both experiments. However, evaluation of tropical analysis and forecast uncertainties do not support such an argument (Podglajen et al., 2014; Žagar, 2017). Total differences partitioned between balanced and unbalanced parts in the NoAeolus and Aeolus analyses show that the two components have similar amplitudes in regions and layers of strong shear, where westerlies shift to easterlies or vice versa. In other regions such as upper troposphere westerlies over Pacific with a weaker KW signal, differences between Aeolus and NoAeolus are almost entirely in balanced modes. Details remain for follow-on investigations using the extended period and sensitivity studies.

4 Discussion and Outlook

Improvements to the KW analyses due to Aeolus data may not come as a surprise since Aeolus winds in the tropics are nearly zonal and tropical improvements have been foreseen (D. G. H. Tan & Andersson, 2004; D. Tan et al., 2007; Žagar, 2004). On the other hand, during the two decades since the Aeolus project started, NWP experienced large advancements with improved data assimilation and more observations used, and the current forecast models routinely run at resolutions around or under 10 km. Yet, practical predictability in extratropics remains under 10 days (Haiden & Coauthors, 2018), and tropics-extratropics interactions are argued as one way to improve medium- and extended-range forecasting (Žagar & Szunyogh, 2020).

Our evaluation of the background fit to other observations shows an overall positive impact of Aeolus winds in the tropics, in spite of large random errors. In fact, the impact in May was larger than for the whole 6-period experiment April-September (not

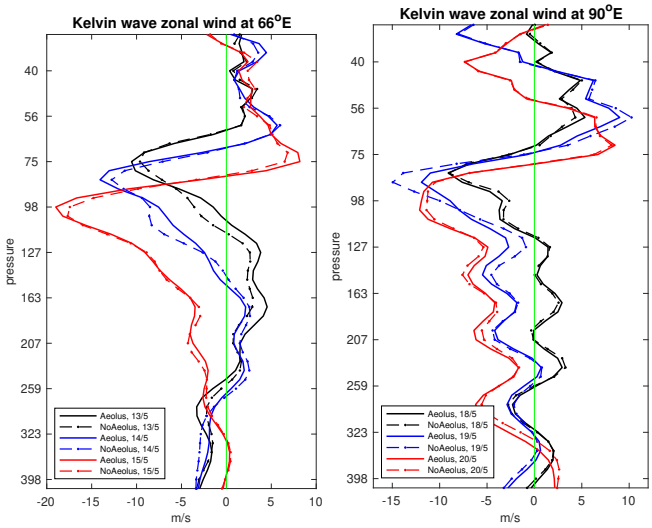

Figure 4. Kelvin wave zonal wind in 12 UTC analyses at three subsequent days in May 2020 in Aeolus (full lines) and NoAeolus (dashed lines) OSEs. The locations are indicated above the panels.

shown). A likely reason is the coupling between the forecast errors and the QBO phase which was stronger in May than in the later part of the OSEs. While the QBO phase and KWs are not explicitly represented in the background-error term for data assimilation in the ECMWF system, the background-error variances are derived using the 4D-Var ensemble of data assimilation thereby accounting for the flow-dependent amplitudes of short-range forecast errors in temperature and winds.

The impact of Aeolus winds on the KWs is closely coupled to the vertical shear lines across TTL and regional aspects of tropical circulation. It remains to investigate how Aeolus winds affect analysis increments in the upper-troposphere and TTL and the dispersiveness of the ensemble prediction system. Here presented results suggest that at least a part of reported forecast improvements in the tropical lower stratosphere (Rennie & Isaksen, 2021) comes from corrections to the large-scale, vertically-propagating Kelvin waves in layers with strong wind shear.

Acknowledgments

We are indebted to the many experts who over years worked on the Aeolus mission until its launch on 22 August 2018, and to many who have been operating the satellite and contributing to the validation and processing of Aeolus measurements at ESA and within the DISC team. The source code of the ECMWF IFS model is not available for public use as it is intellectual property of the ECMWF and its member states. MODES software for the linear wave filtering can be requested through `http://modes.cen.uni-hamburg.de`. Results of the modal decomposition of ECMWF OSEs discussed in the paper are available at `https://zenodo.org/record/4942970#.YMkZVi2B0Q8` (doi: 10.5281/zenodo.4942970). Archiving the input OSE analyses for the presented period in May 2020 to the same repository is underway.

References

Alexander, M. J., & Ortland, D. A. (2010). Equatorial waves in High Resolution Dynamics Limb Sounder (HIRDLS) data. *J. Geophys. Res.*, *115*, D24111. doi: 10

.1029/2010JD014782

Baars, H., Radenz, M., Floutsi, A. A., Engelmann, R., Althausen, D., Heese, B., ... Wandinger, U. (2021). Californian wildfire smoke over Europe: A first example of the aerosol observing capabilities of Aeolus compared to ground-based lidar. *Geophy. Res. Let.*, *48*, e2020GL092194. doi: https://doi.org/10.1029/2020GL092194

Baldwin, M. P., & Coauthors. (2001). The quasi-biennial oscillation. *Rev. Geophys.*, *39*, 179-229.

Banyard, T. P., Wright, C. J., Hindley, N. P., Halloran, G., Krisch, I., Kaifler, B., & Hoffmann, L. (2021). Atmospheric Gravity Waves in Aeolus Wind Lidar Observations. *Geophysical Research Letters*, *48*, e2021GL092756. doi: https://doi.org/10.1029/2021GL092756

Bauer, P., Thorpe, A., & Brunet, G. (2015). The quiet revolution of numerical weather prediction. *Nature*, *525*(47), 10.1038/nature14956. doi: https://doi.org/10.1038/nature14956

Blaauw, M., & Žagar, N. (2018). Multivariate analysis of Kelvin wave seasonal variability in ECMWF L91 analyses. *Atmos. Chem. Phy.*, *18*, 8313-8330. doi: 10.5194/acp-18-8313-2018

ESA. (1999). *Atmospheric Dynamics Mission, Reports for Mission Selections.* ESA SP-1233, 4, 155 pp.

ESA. (2008). *ADM-Aeolus Science Report.* ESA SP-1311, 121 pp.

Fisher, M., Leutbecher, M., & Kelly, G. (2005). On the equivalence between kalman smoothing and weak-constraint four-dimensional variational data assimilation. *Q. J. R. Meteorol. Soc.*, *131*, 3235-3246.

Flannaghan, T. J., & Fueglistaler, S. (2012). Tracking Kelvin waves from the equatorial troposphere into the stratosphere. *J. Geophys. Res.*, *117*. (D21108) doi: 10.1029/2012JD017448

Flannaghan, T. J., & Fueglistaler, S. (2013). The importance of the tropical tropopause layer for equatorial Kelvin wave propagation. *J. Geophys. Res.*, *118*, 5160-5175.

Fujiwara, M., Suzuki, J., Gettelman, A., Hegglin, M., Akiyoshi, H., & Shibata, K. (2012). Wave activity in the tropical tropopause layer in seven reanalysis and four chemistry climate model data sets. *J. Geophy. Res. - Atmospheres*, *117*(D12). (D12105) doi: 10.1029/2011JD016808

Haiden, T., & Coauthors. (2018). *Evaluation of ECMWF forecasts, including the 2018 upgrade.* ECMWF Technical memo 831, October 2018. Available from http://www.ecmwf.int.

Kasahara, A. (2020). *3D Normal Mode Functions (NMFs) of a Global Baroclinic Atmospheric Model.* Modal View Of Atmospheric Variability: Applications Of Normal-Mode Function Decomposition in Weather and Climate Research. N. Žagar and J. Tribbia, Eds., Springer, Mathematics of Planet Earth Series, Vol.8.

Kasahara, A., & Puri, K. (1981). Spectral representation of three-dimensional global data by expansion in normal mode functions. *Mon. Wea. Rev.*, *109*, 37-51.

Kim, H., Caron, J. M., Richter, J. H., & Simpson, I. R. (2020). The Lack of QBO-MJO Connection in CMIP6 Models. *Geophysical Research Letters*, *47*, e2020GL087295. doi: https://doi.org/10.1029/2020GL087295

Kim, J. E., & Alexander, M. J. (2013). Tropical precipitation variability and convectively coupled equatorial waves on submonthly time-scales in reanalyses and TRMM. *J. Climate*, *26*, 3013-3030.

Lean, P., Holm, E. V., Bonavita, M., Bormann, N., McNally, A. P., & Järvinen, H. (2021). Continuous data assimilation for global numerical weather prediction. *Q. J. R. Meteorol. Soc.*, *147*, 273-288.

Matthews, A., & Madden, R. A. (2000). Observed propagation and structure of the 33-h atmospheric Kelvin wave. *J. Atmos. Sci.*, *57*, 3488-3497.

Park, Y.-Y., Buizza, R., & Leutbecher, M. (2004). TIGGE: preliminary results on comparing and combining ensembles. *Q. J. R. Meteorol. Soc.*, *134*, 2029-2050.

Podglajen, A., Hertzog, A., Plougonven, R., & Žagar, N. (2014). Assessment of the accuracy of (re)analyses in the equatorial lower stratosphere. *J. Geophys. Res.*, *119*, 11166-11188.

Reitebuch, O. (2012). *The spaceborne wind lidar mission ADM-Aeolus.* In Atmospheric Physics. Schumann U. (Ed.) Research Topics in Aerospace. Springer, Berlin, Heidelberg, pages 815-827. Retrieved from `https://doi.org/10.1007/978-3-642-30183-4_49`

Rennie, M., & Isaksen, L. (2020). *The NWP Impact of Aeolus Level-2B Winds at ECMWF.* ECMWF Research Department Technical Memorandum 864. Available from http://www.ecmwf.int/en/research/publications. Retrieved from `https://dx.doi.org/10.21957/alift7mhr`

Rennie, M., & Isaksen, L. (2021). The impact of Aeolus wind retrievals in ECMWF global weather forecasts. *Q. J. R. Meteorol. Soc.*, *147*, submitted.

Salby, M. L., & Garcia, R. R. (1987). Transient response to localized episodic heating in the tropics. Part I: Excitation and short-time near-field behavior. *J. Atmos. Sci.*, *44*, 458-498.

Sobel, A., Polvani, N., & Nilsson, J. (2001). The weak temperature gradient approximation. *J. Atmos. Sci.*, *58*, 1473-1489.

Stoffelen, A., Pailleux, J., Källén, E., Vaughan, J. M., Isaksen, L., Flamant, P., ... Ingmann, P. (2005). The atmospheric dynamic mission for global wind measurements. *Bull. Amer. Meteor. Soc.*, *86*, 73-87.

Suzuki, J., & Shiotani, M. (2008). Space-time variability of equatorial Kelvin waves and intraseasonal oscillations around the tropical tropopause. *J. Geophys. Res.*, *113*, D16110. doi: 10.1029/2007JD009456

Suzuki, J., Shiotani, M., & Nishi, N. (2010). Lifetime and longitudinal variability of equatorial Kelvin waves around the tropical tropopause region. *J. Geophys. Res.*, *115*, D03103. doi: 10.1029/2009JD012261

Tan, D., Andersson, E., De Kloe, J., Marseille, G.-J., Stoffelen, A., Denneulin, P. P. M., ... Nett, H. (2008). The ADM-Aeolus wind retrieval algorithms. *Tellus*, *60 A*, 191-205. doi: 10.1111/j.1600-0870.2007.00285.x

Tan, D., Andersson, E., Fisher, M., & Isaksen, L. (2007). Observing-system impact assessment using a data assimilation ensemble technique: application to the ADM-Aeolus wind profiling mission. *Q. J. R. Meteorol. Soc.*, *133*, 381-390.

Tan, D. G. H., & Andersson, E. (2004). *Expected benefit of wind profiles from the ADM-Aeolus in a data assimilation system.* Final report for ESA contract No. 15342/01/NL/MM, October 2004.

Vitart, F., Balsamo, G., Buizza, R., Ferranti, L., Keeley, S., Magnusson, L., ... Weisheimer, A. (2014). *Sub-seasonal predictions.* ECMWF Research Department Technical Memorandum n. 734, pp. 47 (available from ECMWF, Shinfield Park, Reading RG2-9AX, UK).

Šavli, M., Žagar, N., & Anderson, J. (2018). Assimilation of the horizontal line-of-sight winds with a mesoscale EnKF data assimilation system. *Q. J. R. Meteorol. Soc.*, *144*, 2133-2155. doi: 10.1002/qj.3323

Žagar, N. (2004). Assimilation of equatorial waves by line of sight wind observations. *J. Atmos. Sci.*, *61*, 1877-1893.

Žagar, N. (2017). A global perspective of the limits of prediction skill of NWP models. *Tellus A*, *69*, 1317573.

Žagar, N., Andersson, E., Fisher, M., & Untch, A. (2007). Influence of the quasi-biennial oscillation on the ECMWF model short-range forecast errors in the tropical stratosphere. *Q. J. R. Meteorol. Soc.*, *133*, 1843-1853.

Žagar, N., Blaauw, M., Jesenko, B., & Magnusson, L. (2016). *Diagnosing model performance in the tropics* (Vol. 147). ECMWF Newsletter, available from http://www.ecmwf.int/publications/newsletters.

Žagar, N., Buizza, R., & Tribbia, J. (2015). A three-dimensional multivariate modal analysis of atmospheric predictability with application to the ECMWF ensemble. *J. Atmos. Sci.*, *72*, 4423-4444.

Žagar, N., Isaksen, L., Tan, D., & Tribbia, J. (2013). Balance properties of the short-range forecast errors in the ECMWF 4D-Var ensemble. *Q. J. R. Meteorol. Soc.*, *139*, 1229-1238.

Žagar, N., Kasahara, A., Terasaki, K., Tribbia, J., & Tanaka, H. (2015). Normal-mode function representation of global 3D datasets: open-access software for the atmospheric research community. *Geosci. Model Dev.*, *8*, 1169-1195.

Žagar, N., & Szunyogh, I. (2020). Comments on "What Is the Predictability Limit of Midlatitude Weather?". *J. Atmos. Sci.*, *72*(2), 781-785. doi: https://doi.org/10.1175/JAS-D-19-0166.1

Wallace, J. M., & Kousky, V. E. (1968). Observational evidence of Kelvin waves in the tropical stratosphere. *J. Atmos. Sci.*, *25*, 900-907.

Wheeler, M., & Kiladis, G. N. (1999). Convectively coupled equatorial waves: analysis of clouds and temperature in the wavenumber-frequency domain. *J. Atmos. Sci.*, *56*, 374-399.

Zhang, C. (2005). Madden-Julian oscillation. *Rev. Geophys.*, *43*, 1-36.

Tropical analysis uncertainties and Kelvin waves: what can be learnt from the Aeolus wind profiles?

N. Žagar[1], M. Rennie[2]and L. Isaksen[2]

[1]Meteorologisches Institut, Universität Hamburg, Germany

[2]European Centre for Medium Range Weather Forecasts, Reading, UK

An example of the Kelvin wave filtering in the ECMWF model

The Kelvin wave is the slowest eastward-propagating linear wave on the sphere. Its horizontal structure is represented in terms of Hough harmonics whereas the vertical structure is obtained by numerically solving the vertical structure equation for the realistic stability and discretization profiles for the troposphere and stratosphere (Kasahara, 2020; Blaauw & Žagar, 2018; Castanheira & Marques, 2015). Its filtering in operational ECMWF forecasts using the MODES software (Žagar et al., 2015) has been routinely performed since 2014, currently at `https://modes.cen.uni-hamburg.de`. An example of Kelvin wave in the ECMWF model forecasts is shown in Fig. S1 for a single deterministic forecast by the operational system in May 2020 that assimilated Aeolus winds. Forecasts at subsequent days show the vertical KW propagation according to classical linear theory (Andrews et al., 1987). A horizontal line near 33 hPa is added for an easier

visualization of the downward moving wave phase wind over the Indian ocean sector, in evidence of the vertical propagation of energy. The high vertical resolution of the operational ECMWF model resolves an eastward-slanted wave structure in TTL and in the stratosphere. Recent studies of the KW variability using three-dimensional linear theory include Blaauw and Žagar (2018), who described seasonal variability of KWs in TTL in relation to the background winds and stability in ECMWF operational analyses, and Castanheira and Marques (2015), who analyzed KWs coupled to convection.

Other supporting Figures

Tropical zonal winds in the Aeolus and NoAeolus analyses along with their portions associated with the Rossby (or balanced) and non-Rossby (or unbalanced) modes are shown in Figures S2-S4.

References

Andrews, D. G., Holton, J. R., & Leovy, C. B. (1987). *Middle atmosphere dynamics.* Academic Press, Inc.

Blaauw, M., & Žagar, N. (2018). Multivariate analysis of Kelvin wave seasonal variability in ECMWF L91 analyses. *Atmos. Chem. Phy.*, *18*, 8313-8330. doi: 10.5194/acp-18-8313-2018

Castanheira, J., & Marques, C. (2015). Convectively coupled equatorial-wave diagnosis using three-dimensional normal modes. *Quarterly Journal of the Royal Meteorological Society*, *141*(692), 2776–2792. doi: 10.1002/qj.2563

Kasahara, A. (2020). *3D Normal Mode Functions (NMFs) of a Global Baroclinic Atmo-*

spheric Model. Modal View Of Atmospheric Variability: Applications Of Normal-Mode Function Decomposition in Weather and Climate Research. N. Žagar and J. Tribbia, Eds., Springer, Mathematics of Planet Earth Series, Vol.8.

Žagar, N., Kasahara, A., Terasaki, K., Tribbia, J., & Tanaka, H. (2015). Normal-mode function representation of global 3D datasets: open-access software for the atmospheric research community. *Geosci. Model Dev.*, *8*, 1169-1195.

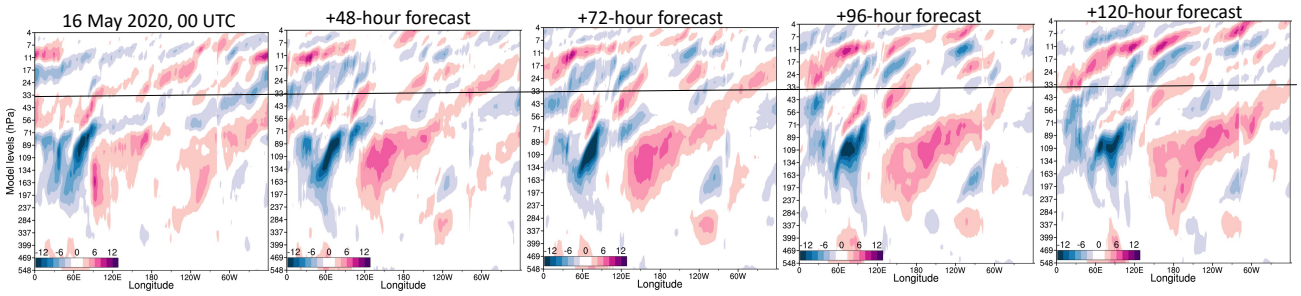

Figure S1. Kelvin wave zonal wind in the operational ECMWF analysis on 16 May 2020, 00 UTC, and in 48-hour, 72-hour, 96-hour and 120-hour forecasts. The zonal wind is averaged over the equatorial belt 15^o S $-$ 15^o N. Easterlies are in blue and westerlies are in red shades as defined by the colorbar with contouring every 2 m/s. Zero contour is omitted. From `https://modes.cen.uni-hamburg.de`.

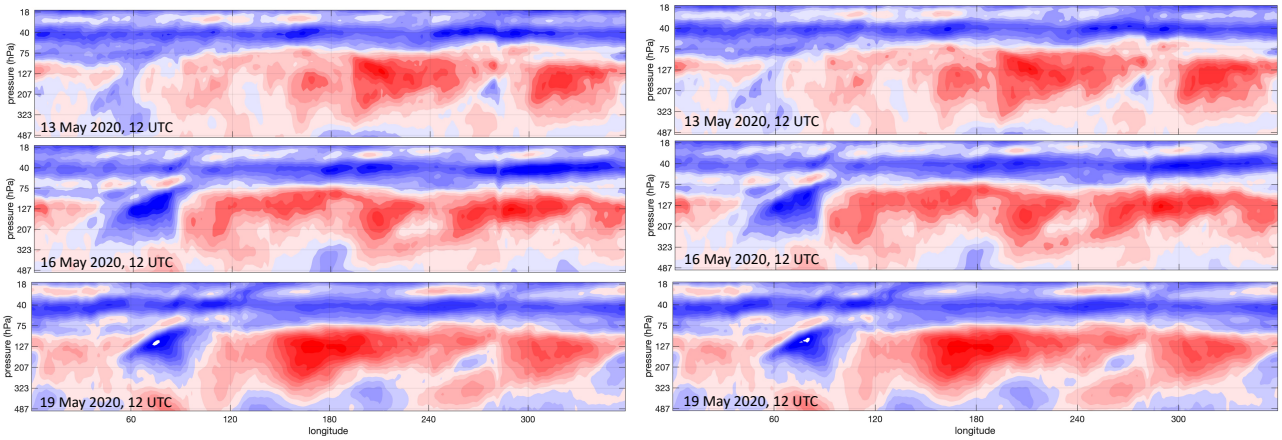

Figure S2. Zonal winds along the equator, averaged over the belt 10^oN-10^oS in (left) NoAeolus and (right) Aeolus experiments on 13 May, 16 May and 19 May 2020, 12 UTC. Shading is every 3 m/s, with red shades for westerly winds, and blue shades for easterlies.

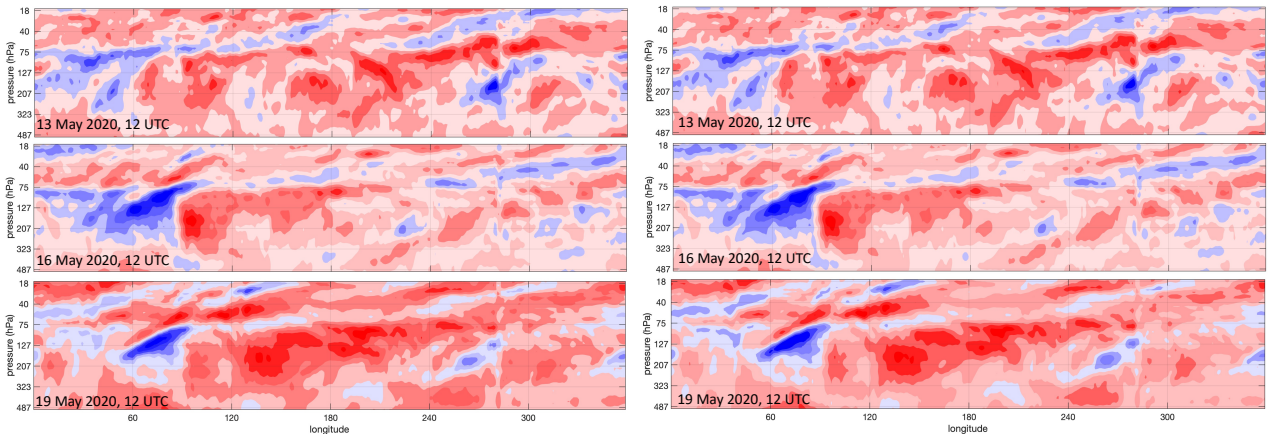

Figure S3. As in Fig. S2 but for the unbalanced (or non-Rossby) zonal winds including the Kelvin and mixed Rossby-gravity zonal winds.

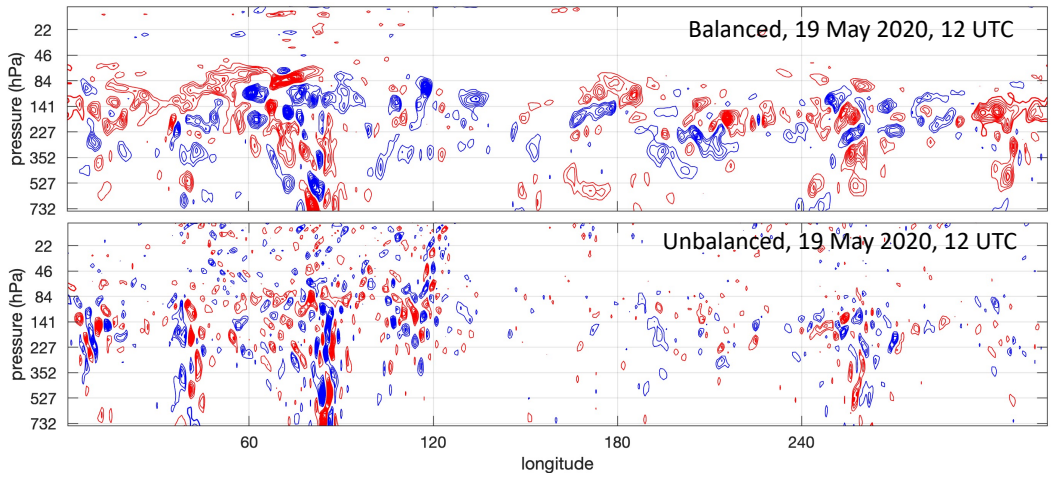

Figure S4. Differences along the equator between the zonal wind in analyses with and without Aeolus winds on 19 May 2020, 12 UTC. Differences are computed separately for balanced (Rossby) and unbalanced (non-Rossby) modes. Contouring is every 0.5 m/s, starting at ±1 m/s. Red contours for positive, and blue for negative differences.